Kinetic structure of the sharp injection/dipolarization front in the flow-braking region

V. Sergeev,[1] V. Angelopoulos,[2] S. Apatenkov,[1] J. Bonnell,[3] R. Ergun,[4] R. Nakamura,[5] J. McFadden,[3] D. Larson,[3] and A. Runov[2]

Received 28 August 2009; revised 2 October 2009; accepted 15 October 2009; published 10 November 2009.

[1] Observations of three closely-spaced THEMIS spacecraft at 9–11 Re near midnight and close to the neutral sheet are used to investigate a sharp injection/dipolarization front (SDF) propagating inward in the flow-braking region. This SDF was a very thin current sheet along the North-South direction embedded within an Earthward-propagating flow burst. A short-lived depression of the total magnetic field (down to 1 nT), devoid of wave activity and intense particle fluxes, stays ahead of the SDF. Clear finite proton gyroradius effects, which help visualize the geometry and sub-gyroscale of the SDF, are seen centered at the thin current sheet. The SDF nearly coincides with the narrow interface between plasmas of different densities and temperatures. At that interface, we observed strong (40–60 mV/m peak) E-field bursts of the lower-hybrid time scale that are confined to a localized region of density depletions. This sharp dipolarization/injection front propagating in the flow-braking region appears to be a complicated kinetic-scale plasma structure that combines a number of small-scale elements (Bz drops, thin current sheets, LH cavities, injection fronts) previously discussed as separate objects.
Citation: Sergeev, V., V. Angelopoulos, S. Apatenkov, J. Bonnell, R. Ergun, R. Nakamura, J. McFadden, D. Larson, and A. Runov (2009), Kinetic structure of the sharp injection/dipolarization front in the flow-braking region, *Geophys. Res. Lett.*, *36*, L21105, doi:10.1029/2009GL040658.

1. Introduction

[2] Most of the plasma, flux, and energy in the plasma sheet is transferred from the magnetotail by narrow, fast-flowing streams known as bursty bulk flows (BBFs) [*Angelopoulos et al.*, 1994]. The final stage in their evolution, however, continues to be a subject of considerable debate. Interaction between the flow and the strong near-Earth magnetic field is thought to be important in generation of the substorm current wedge and auroral breakup [*Ohtani*, 2004]. Although BBF-associated flux transport was observed to be nearly continuous from the midtail to ~12–15 Re, its rate decreased in the transition area between the dipole-like and magnetotail-like field (around 10 Re [*Schödel et al.*, 2001]). Therefore, a significant number of fast-flow events do not penetrate deeply into the inner magnetosphere [*Takada et al.*, 2006]. Although interaction of the injected plasma with the ambient plasma is an important aspect of fast-flow evolution, it has not been investigated adequately. In particular, the shortage of multi-point, high-resolution observations in the flow-braking region has been until recently a major observational obstacle. The THEMIS project [*Angelopoulos*, 2008], with its three closely-spaced inner-magnetospheric probes, measures routinely the flow-braking region and returns data at a high rate during frequent burst-mode observation intervals. In this paper we report on a flow-burst episode when three THEMIS probes were in a favorable spatial configuration to track propagation of a sudden injection/dipolarization front (SDF) and resolve its sub-gyroscale structure for the first time.

2. Observations

[3] We use observations from the magnetometer (FGM), the particle spectrometers (ESA and SST), and the electric field double probe (EFI) instruments on the THEMIS probes described by *Angelopoulos* [2008, and references therein].

[4] On 23 February 2008 at ~07:08 UT, the onset of a weak but distinct substorm event with a magnetic bay of ~150 nT was observed at Ft. Smith. Distinct Pi2 pulsations and an 0.1 MA substorm current wedge perturbations were observed at midlatitude stations. The three innermost THEMIS probes (P3, P4, and P5) near the neutral sheet ($|Bx| < Bz$, see Figure 1), formed a triangle with the P3 probe at [−11.31; 1.73; −2.71] GSM and the P4 probe at [−11.13; 2.63; −2.75]. The P5 probe, at [−9.29; 1.25; −2.59], was 2 Re earthward of P3 and P4. Prior to (and throughout) the event, the Bz component and the plasma pressure values at P5 were 1.5 times larger than those at P3 and P4, indicating that the probes observed a steady Earthward gradient of magnetic and plasma pressures at the periphery of the inner magnetosphere. The plasma beta parameter was high; it never fell below 3 during the period of interest.

[5] The spin-resolution data in Figure 1 show significant increases in Bz, indicating passage of a sudden dipolarization front (SDF) preceded by a brief Bz dip (depression). Even though there was about 53 sec of delay between the SDF signatures at P3 and P4 and those at the innermost

[1]Institute of Physics, St. Petersburg State University, Saint Petersburg, Russia.
[2]Department of Earth and Space Sciences and Institute of Geophysics and Planetary Physics, University of California, Los Angeles, California, USA.
[3]Space Science Laboratory, University of California, Berkeley, California, USA.
[4]Laboratory for Atmospheric and Space Physics, Boulder, Colorado, USA.
[5]Space Research Institute, Austrian Academy of Sciences, Graz, Austria.

0094-8276/09/2009GL040658$05.00

probe (P5), all indicated that the SDF had similar shape and intensity. Using fast-survey (0.25 sec resolution) data, we applied minimum variance analysis (MVA) to the time intervals between the Bz peaks, which gave us well-defined directions of the eigenvector N3 (with middle-to-minimal eigenvalue ratios L2/L3 – 29., 32., and 7.5 for 28, 16, and 16 data points, at P3, P4, and P5, respectively). The N3 vectors (in GSM coordinates) are [0.95; 0.04; 0.30] at P3, [0.93; 0.09; 0.34] at P4, and [0.94; −0.21; 0.24] at P5. Interpreting these vectors as normal to the current sheet plane implies that near the neutral sheet, the SDF is a vertical, thin current sheet with a plane nearly perpendicular to the radial direction, as shown at the top of Figure 1. Let us test this conclusion and determine the scale and structure of the SDF using plasma data.

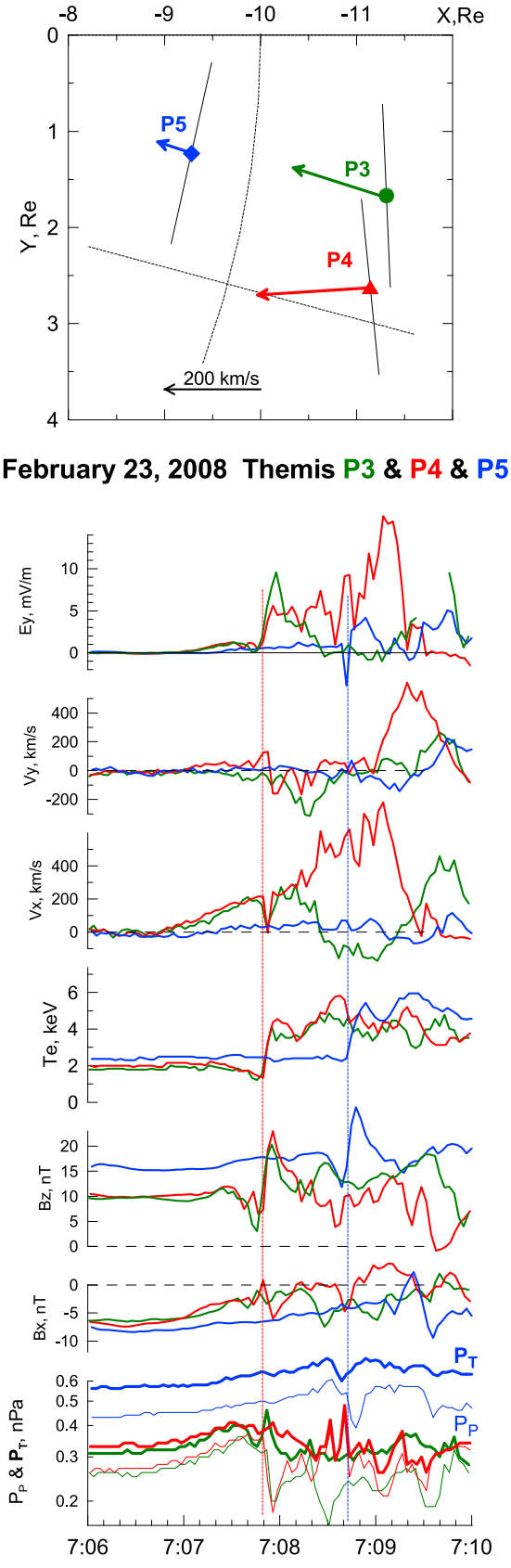

Figure 1. (top) Configuration of three THEMIS spacecraft in the XY plane with superimposed r = const and MLT coordinate lines at 07:08 UT on 23 February 2008; arrows show the ion velocity vectors measured just prior to SDF passage; SDF front orientation as inferred from MVA analysis is shown. (bottom) Spin-average parameters measured at three probes (from bottom to top): plasma and total pressures (Pp - thin lines, Pt - thick lines); Bx- and Bz magnetic field components; electron temperature Te; Vx and Vy components of total ion velocity; Ey field from the EFI instrument.

[6] As shown in Figure 1, prior to SDF passage and after 07:06:50 UT, the three probes observed a smooth increase in the plasma flow Vx component with a simultaneous increase in plasma and total pressure. Such increases, which suggest a sheath-like interaction between the ambient plasma and a localized structure intruding from the magnetotail, are common at the periphery of the dipole-like inner magnetosphere. Just before the SDF, the Vx flow velocity was 180–200 km/s at the P3 probe and 200–220 km/s at the P4 probe. Simultaneous SDF recording at P3 and P4 showed that the intersection of the vertical SDF front with the neutral sheet was aligned azimuthally; therefore, the 53 s time delay to P5 gives an average inward SDF propagation velocity of Vxt = 220 km/s, in good agreement with flow measurements and roughly four times smaller than the fast mode velocity. The observed flow velocity and the Ey-flux transport rate at P5 are three times smaller (peak Vx ∼ 70 km/s), indicating that the SDF structure is indeed decelerating in the flow-braking region.

[7] As the SDF passes by, the plasma energy increases (for example, Te doubles from 2 keV to 4 keV in Figure 1), and the density and plasma pressure decrease. More details on the plasma response at P5 are shown in Figure 2. Both electron and proton components change at the SDF, which separates pre-SDF cold, dense, ambient plasma with bi-directional electron pitch-angle distributions from post-SDF hot plasma with either isotropic or pancake-like electron distributions. The very sharp transition in electron properties at the SDF occurred within one spin period (3 sec). The zigzag pattern in the top plots, which represents changes in proton energy flux angular distributions with time in P5's rotational plane (∼GSE X, Y plane), illustrates how this boundary approaching from the magnetotail was sensed remotely due to the proton finite gyroradius. *Angelopoulos et al.* [1999] have made similar observations for the hot component. Here, for the first time, both (cold and hot) populations were seen simultaneously; they came from different arrival angles, so they did not mix. The duration of the zigzag pattern increased with particle velocity,

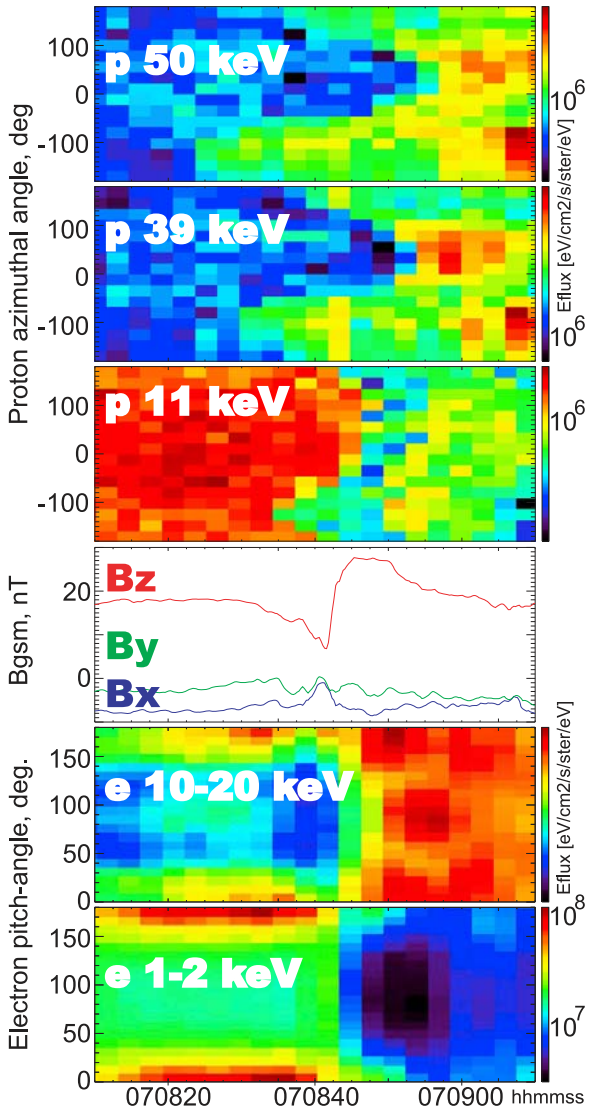

Figure 2. (top) Proton energy flux variations in three energy ranges as a function of flux direction in probe rotation (∼ecliptic) plane; 0 deg and 90 deg correspond to the Earthward and duskward flux, respectively. (middle) GSM magnetic field components; (bottom) electron energy flux variation in two energy ranges as function of pitch angle.

changing from dt ∼ 15 sec at 11keV to dt ∼ 30 sec at 50 keV. Estimating the local Earthward propagation velocity of this structure as 2 Rci/dt (with ion gyroradius Rci ∼ 760 km and 1600 km for energies 11 and 50 keV respectively, calculated in average B = 20 nT), gives 80–100 km/s as the inward propagation velocity. This is in agreement with the local ion flow velocity (70 km/s) measured at P5 in front of the SDF. The peaks of the zigzag pattern are, however, shifted by approx. −30° from their nominal directions (±90° in the ecliptic plane), suggesting that normal to this structure deviated ∼30° dawnward from the solar direction.Such a shift is in qualitative agreement with the front orientation derived from MVA (Figure 1). The finite-gyroradius pattern is especially distinct at P5 because of the slow local plasma flow there. However, it can still be discerned at P3 and P4 despite the strong, flow-related anisotropy (not shown).

[8] The remote sensing pattern in Figure 2 illustrates that the scale-size of the SDF is small compared to the ion gyroradius. Taking the SDF velocity to be 80 km/s, the 4 sec duration of the Bz rise (peak-to-peak) gives an SDF thickness of about 300 km, about a half the gyroradius of the thermal ion (with a temperature of 6 to 8 keV as measured in a 20 nT magnetic field) before/after the SDF.

[9] Figure 3 is a close-up view of the injection/dipolarization front using burst mode magnetic and electric field data available at 128 Hz time resolution. A notable feature of SDF crossings at all three probes is the high-amplitude EF wave/burst packet with peak amplitudes between 40 and 60 mV/m. Its total duration is between 1 and 2 sec, so it occupies only a fraction of the SDF and always stays closer to the SDF Bz peak. The highest intensity is observed in deepest density depletions indicated by the drops in electric probe potentials. The characteristic time scales of these bursts/waves were about 0.150 sec at P4 (between 07:07:51.1 and 07:07:53 UT), 0.05–0.1 sec at P3 (between 07:07:51.3 and 07:07:52.1 UT), and about 0.1 sec at P5 (between 07:08:42.7 and 07:08:43.8 UT); they are about the low-hybrid time scale, f_{LH} is 13 Hz for B = 20 nT and N = 0.3 cm^{-3}. The E-wave amplitude perpendicular to B is larger than the parallel component, the magnetic field perturbations on that time scale are weak (≪1 nT), so the waves could be largely electrostatic for such high E-field magnitudes. The E-field appearance, which is wave-like at P3 and P5, resembles a sequence of individual spikes (associated with narrow density drops) at the P4 probe.

[10] Such an intense E-field may be related to particle energization. We use the electron flux measured in near-equatorial sectors by the rotating particle detector 16 times per spin. Since electrons are fast and very likely gyrotropic, this technique gives the most accurate timing of electron acceleration when measuring near the equator in a nearly vertical (B ∼ Bz) magnetic field. A comparison of electron energy fluxes measured below (1–3 keV) and above the electron energy spectrum peak (for 10–30 keV) shows that main energy change was short-lived (<1 sec for P3, P4), and occurred at the same location as intense electric LH waves and bursts. Therefore, the intense E-field structure stays at the interface between relatively cold, dense, ambient plasma and hot, rarefied injected plasma. The electron flux does not follow the time profile of magnetic field change and is thus inconsistent with a simple version of betatron acceleration.

[11] A survey of SDFs observed under similar conditions confirms that most results presented (vertical, thin current sheets, ion gyroradius pattern similar to Figure 2, localized density depletion containing intense E-waves and coincident with sharp electron temperature change) have been commonly observed in such short-duration (a few second-long) SDF events.

3. Discussion and Summary

[12] Our analysis focuses on the scale-size, geometry, and especially the structure of the injection/dipolarization front as it appeared in the high-beta equatorial flow-braking region of the magnetotail. The finite-ion-gyroradius pattern in Figure 2 illustrates the sub-ion-gyroradius scale size of

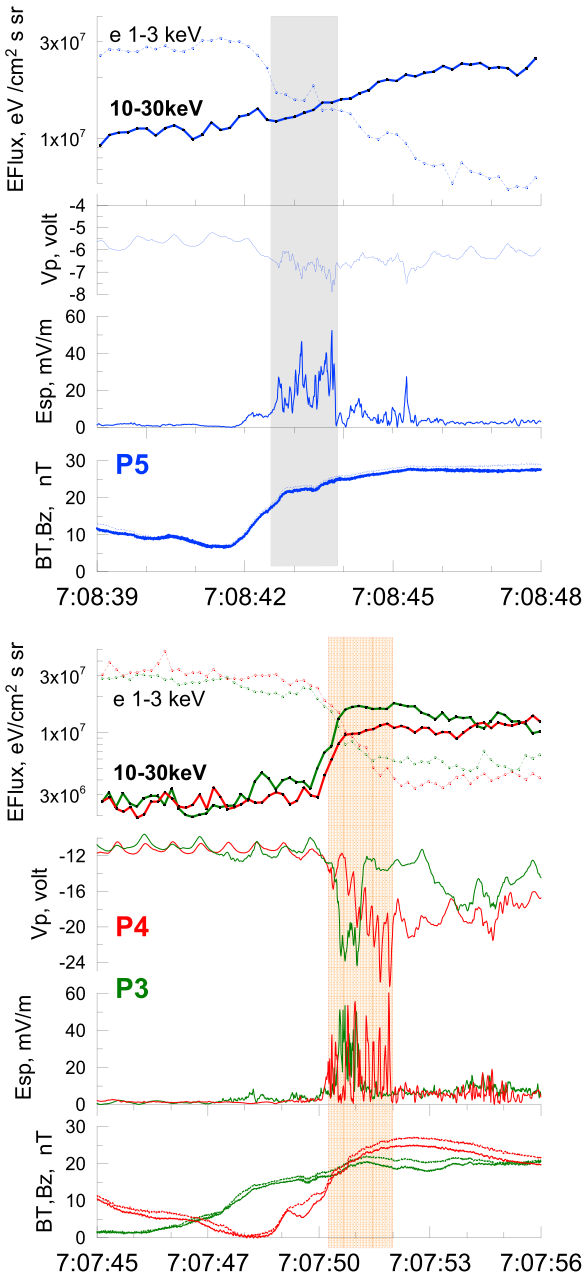

Figure 3. Closeup view of electromagnetic field parameters and electron energy flux variations at the sudden dipolarization fronts; (top) inner probe (P5), (bottom) outer probes (P3 and P4). Each plot includes: total B and GSM Bz component at high time resolution; electric field magnitude in the probe spin plane (Esp) and average potential of booms 1 and 2 (Vp), both at 128 Hz sampling rate; electron energy flux at low (1–3 keV) and high (10–30 keV) energies from rotating detector looking at the spin plane. The hatched strip marks the time interval of strong E-field spikes exceeding 20 mV/m.

this compound structure and provides an additional tool for verifying SDF orientation and propagation direction. With support from MVA, it confirms that the overlapping thin current sheet (dipolarization front) and the thin boundary between cold and hot plasma populations (injection front) stayed vertical near the center of the magnetotail current sheet. This result agrees with previous results obtained tailward of the flow-braking region [e.g., *Nakamura et al.*, 2002; *Runov et al.*, 2009] and implies a thin interface (tangential discontinuity) separating the ambient and injected plasmas, which follows the field line and therefore stays vertical in the center of the tail current sheet.

[13] A narrow Bz decrease preceding sharp dipolarization, sometimes referred to as the explosive growth phase feature [*Ohtani*, 2004], is also common in the plasma sheet [*Ohtani et al.*, 2004]. Near the neutral sheet, the total B magnitude was observed to become as small as 1 nT at P3 and P4. The duration of the magnetic field decrease is short (<3 sec) at P4 and P5. No specific wave activity or special particle distribution features, such as found by *Shiokawa et al.* [2005], were observed. These observations probably represent a plasma structure in near equilibrium. How it is generated and its connection to the dipolarization front are unknown. We note that the SDF's characteristic Bz profile (short drop, then quick increase in the Bz-component) is not limited to the flow-braking region; it is probably formed in front of fast flows in the tail plasma sheet [*Ohtani et al.*, 2004], where its sub-gyro scale thickness has recently been noted by *Runov et al.* [2009].

[14] The most notable new observation from P3, P4, and P5 (Figure 3) is the coincidence of the injection front with a density depletion, which was correlated with a high-amplitude E-field bursts or waves in the lower hybrid frequency range. The phenomenon looks somewhat similar to the lower hybrid solitary structures (or LH cavities, LHC), which were studied mostly at low altitudes in strong magnetic fields [*Schuck et al.*, 2003], but were also identified in the inner magnetosphere by Cluster [*Tjulin et al.*, 2004]. These LHCs are, however, an order of magnitude weaker. Very strong E-fields exceeding 100 mV/m have been reported near the reconnection separatrices [*Cattell et al.*, 2005]. Waves in the substorm-time plasma sheet at 10–15 Re are weaker (up to 5–10 mV/m [*Sigsbee et al.*, 2002]), or a few mV/m [*Shiokawa et al.*, 2005]. Recent work by *Ergun et al.* [2009] demonstrates a wealth of strong wave/burst electric activities during BBFs and dipolarizations as well as the great potential of THEMIS studies. The SDF-related structures in our study have intense LH waves mounted at the boundary between the ambient and bubble plasmas as a part of the Earthward-propagating spatial structure. This suggests a number of questions for future studies, including - what is the role of LH waves in particle acceleration?, and what is the role of contact phenomena in generation of intense LH bursts/waves?

[15] A somewhat similar Cluster observation of the ion-gyro-scale boundary between the hot (inward) and colder (outward) plasma populations, which showed a finite ion-gyroradius pattern, strong E-spikes of tens of mV/m and density depletions at the plasma boundary, and field-aligned currents, was reported by *Sergeev et al.* [2003]. According to their interpretation, a sharp boundary between ring current-like hot plasma and colder plasma sheet plasma formed after the BBF intrusion. Their observations, however, were made in the strong B-field region in the high-latitude portion of the Cluster trajectory throughout the horns of the plasma sheet. Because the relationship of these observations to dipolarizations and the equatorial mapping

of such structures are difficult to establish reliably, it is unclear whether these Cluster observations represent the same plasma object as discussed herein.

[16] The last comment concerns flow-braking. The P3, P4, and P5 observations were performed in the flow-braking region, which is characterized by a steady Earthward gradient of equatorial B-field and plasma pressure. The threefold decrease in SDF propagation velocity from P3/P4 to P5 (from Vx $\sim$ 200 km/s to $\sim$70 km/s, obtained both from plasma moments and from the time scale of ion-gyroradius pattern of Figure 2, top) signifies a deceleration of the SDF structure in the $\sim$2 Re radial distance between these probes. The basic SDF features show little degradation, however. Possible signatures of their braking-related evolution could include an increase in B-minimum values in the dropout just prior to the SDF (from $\sim$1 nT at P3 and P4 to 7 nT at P5) and a decrease in density depletion amplitude at P5 (compare probe potential patterns in Figure 3). SDF passage over the inner probe, P5, mostly decreased the low energy population without changing the high-energy electron flux dramatically; this was not so with passage over P3 and P4. One may also notice some dawnward rotation of the flow vector at P5 compared to the P3, P4 (Figure 1) and a pancake electron distribution at P5 (Figure 2, bottom) after the dipolarization front. This can be contrasted with the pitch-angle distributions at P3,P4, which remained bidirectional and field-aligned, just as they were prior to SDF passage (not shown here).

[17] In conclusion, observations of a sharp dipolarization front propagating throughout the flow-braking region in the high-beta neutral sheet portion of the near midnight plasma sheet, provide the first evidence of the complicated structure and sub-gyro scale of this inherently kinetic plasma boundary separating ambient plasma from injected, low-density, high-temperature plasma. The existence of a high-amplitude E-field in the LH frequency domain in a density depletion at the sharp boundary between ambient and injected bubble plasma makes the SDF an intriguing plasma structure to study further. The extended THEMIS mission, with its clustered, multi-probe configuration in the region of interest, and its high-rate, burst-mode data acquisition, has great potential to advance our understanding of this new object.

[18] **Acknowledgments.** We acknowledge NASA contracts NAS5-02099 and NNX08AD85G, the German Ministry for Economy and Technology and the German Center for Aviation and Space (DLR), contract 50 OC 0302. The work by VS and SA was supported by Russian Ministry of Education and Science grants and by RFBR grants 07-02-91703 and 10-05-00223. We thank Judy Hohl for help with the manuscript preparation.

References

Angelopoulos, V. (2008), The THEMIS mission, *Space Sci. Rev.*, *598*, 5, doi:10.1007/s11214-008-9336-1.

Angelopoulos, V., C. F. Kennel, F. V. Coroniti, R. Pellat, M. G. Kivelson, R. J. Walker, C. T. Russell, W. Baumjohann, W. C. Feldman, and J. T. Gosling (1994), Statistical characteristics of bursty bulk flow events, *J. Geophys. Res.*, *99*, 21,257.

Angelopoulos, V., F. S. Mozer, T. Mukai, K. Tsuruda, S. Kokubun, and T. J. Hughes (1999), On the relationship between bursty flows, current disruption and substorms, *Geophys. Res. Lett.*, *26*, 2841.

Cattell, C., et al. (2005), Cluster observations of electron holes in association with magnetotail reconnection and comparison to simulations, *J. Geophys. Res.*, *110*, A01211, doi:10.1029/2004JA010519.

Ergun, R. E., et al. (2009), Observations of double layers in Earth's plasma sheet, *Phys. Rev. Lett.*, *102*, 155002, doi:10.1103/PhysRevLett.102.155002.

Nakamura, R., et al. (2002), Motion of the dipolarization front during a flow burst event observed by Cluster, *Geophys. Res. Lett.*, *29*(20), 1942, doi:10.1029/2002GL015763.

Ohtani, S.-I. (2004), Flowbursts in the plasma sheet and auroral substorm onset: Observational constraints on connection between midtail and near-Earth substorm processes, *Space Sci. Rev.*, *113*, 77.

Ohtani, S., M. A. Shay, and T. Mukai (2004), Temporal structure of the fast convective flow in the plasma sheet: Comparison between observations and two-fluid simulations, *J. Geophys. Res.*, *109*, A03210, doi:10.1029/2003JA010002.

Runov, A., V. Angelopoulos, M. I. Sitnov, V. A. Sergeev, J. Bonnell, J. P. McFadden, D. Larson, K.-H. Glassmeier, and U. Auster (2009), THEMIS observations of an earthward-propagating dipolarization front, *Geophys. Res. Lett.*, *36*, L14106, doi:10.1029/2009GL038980.

Schödel, R., W. Baumjohann, R. Nakamura, V. A. Sergeev, and T. Mukai (2001), Rapid flux transport in the central plasma sheet, *J. Geophys. Res.*, *106*, 301.

Schuck, P. W., J. W. Bonnell, and P. M. Kintner (2003), A review of lower hybrid solitary structures, *IEEE Trans. Plasma Sci.*, *31*, 1125.

Sergeev, V. A., J.-A. Sauvaud, H. Reme, A. Balogh, P. Daly, Q.-G. Zong, V. Angelopoulos, M. Andre, and A. Vaivads (2003), Sharp boundary between the inner magnetosphere and active outer plasma sheet, *Geophys. Res. Lett.*, *30*(15), 1799, doi:10.1029/2003GL017095.

Shiokawa, K., Y. Miyashita, I. Shinohara, and A. Matsuoka (2005), Decrease in Bz prior to the dipolarization in the near-Earth plasma sheet, *J. Geophys. Res.*, *110*, A09219, doi:10.1029/2005JA011144.

Sigsbee, K., C. A. Cattell, D. Fairfield, K. Tsuruda, and S. Kokubun (2002), Geotail observations of low-frequency waves and high-speed earthward flows during substorm onsets in the near magnetotail from 10 to 13 RE, *J. Geophys. Res.*, *107*(A7), 1141, doi:10.1029/2001JA000166.

Takada, T., R. Nakamura, W. Baumjohann, Y. Asano, M. Volwerk, T. L. Zhang, B. Klecker, H. Reme, E. A. Lucek, and C. Carr (2006), Do BBFs contribute to inner magnetosphere dipolarizations: Concurrent Cluster and Double Star observations, *Geophys. Res. Lett.*, *33*, L21109, doi:10.1029/2006GL027440.

Tjulin, A., M. Andre, A. I. Eriksson, and M. Maksimovich (2004), Observations of lower hybrid cavities in the inner magnetosphere by the Cluster and Viking satellites, *Ann. Geophys.*, *22*, 2961.

V. Angelopoulos and A. Runov, Institute of Geophysics and Planetary Physics, University of California, 3845 Slichter Hall, Los Angeles, CA 90095, USA.

S. Apatenkov and V. Sergeev, Institute of Physics, St. Petersburg State University, Ulyanovskya 1, Saint Petersburg 198504, Russia.

J. Bonnell, D. Larson, and J. McFadden, Space Science Laboratory, University of California, 7 Gauss Way, Berkeley, CA 94720, USA.

R. Ergun, Laboratory for Atmospheric and Space Physics, Campus Box 530, 1234 Innovation Dr., Boulder, CO 80303, USA.

R. Nakamura, Space Research Institute, Austrian Academy of Sciences, Schmiedlstr. 6, A-8042 Graz, Austria.